

Quadrature properties of high harmonics emitted by two-level atom

Ákos Gombkötő¹

¹*Department of Theoretical Physics, University of Szeged, Tisza Lajos körút 84, H-6720 Szeged, Hungary*

We analyse the quadrature mean values and variances of high harmonic photons, emitted by a classically driven elementary quantum source of radiation. This fundamental system is modelled with a two-level atom. The quadrature mean values and variances are calculated for harmonic modes in the near-field. Numerical results imply the presence of weak squeezing in each harmonic mode, more pronounced in even harmonics. Approximate time-evolution of the collective electromagnetic field is calculated, and the electric field-variance of the scattered pulse-train is given.

PACS numbers: 42.65.Ky, 42.50.Ar

I. INTRODUCTION

Attosecond pulses push the limits of high-precision measurement to unprecedented scales. Historically, attosecond science has used models which treat the electron quantum-mechanically, and the electromagnetic field classically [10, 12, 13]. This description naturally can not capture all characteristics of the process. Generation of attosecond pulses is made possible mainly by high harmonic generation, a strongly nonlinear optical effect that plays central role in attosecond physics [5, 6, 12].

In previous work our calculations implied nonclassical features of high-harmonic photons, including sub-Poissonian photon statistics of the even harmonics and the anticorrelation between even- and odd-harmonics. Depending on the phenomena one wishes to investigate, modelling attosecond pulses as classical radiation –i.e. in coherent quantum state– may be insufficient, and its quantum properties turn out to be important. In this paper, we will describe the quadrature properties of the quantized harmonics modes individually, and treat the collective scattered radiation separately.

Closely connected to quadrature variance, the concept of squeezed light is a historically important idea. Not only fundamental, but also applied science have benefited a lot from using squeezed light, being a valuable tool of metrology and for quantum information processing. Both the degree of squeezing and the squeezing bandwidth are important for potential applications. Current experiments with pulsed squeezed light reach a bandwidth up to tens of THz [9]. Sub shot-noise measurements in spectroscopy, sub-wavelength image discerning and recording are just a few examples [2, 16, 21]. It has also been proposed that strong intensity fluctuations can enhance multi-photon processes compared to classical light of the same intensity [7]. Significant increase in lateral displacement measurement has been demonstrated in [19], using squeezed beams. Recently it has become possible to generate and analyse time-locked patterns of quadrature squeezed noise, through sampling with femtosecond pulses in a non-destructive manner [17].

To date, most balanced homodyne detection measurements have been performed in the frequency domain,

where in practice any measurement of the field integrates over some sideband spectrum. A light field is often analysed with respect to many different modulation frequencies, and the result constitutes a spectrum, [3] where in principle every modulation mode can be in a different quantum state. We note that standard homodyne detection suffers from significant bandwidth limitation: While the bandwidth of optical states can easily span many THz, homodyne detection is inherently limited to the electrically accessible, MHz to GHz range, leaving a significant gap between the relevant optical phenomena and the measurement capability. This can be lifted by using parallel homodyne measurement [18].

II. MODEL

The model of the material system is a two-level system, which may be an acceptably used to describe harmonic generation in semiconductor heterostructures [8], granted that the wavefunction is spams basically two band, with negligible additional components. On the other hand, the simplicity of two-level systems help forming qualitatively correct predictions, and offer insight into the dynamics.

In our model, we will assume that the external excitations are strong, and can be treated classically, and that the dipole-approximation during interaction stands. We separate the electromagnetic field into far-field and near-field regions, and express the far-field scattered radiation with the near-field quantities, which are calculated approximately, without taking spatial dependencies into consideration.

For this purpose, the far-field vector potential operator can be expressed [11] with the current density operator as:

$$A(\mathbf{r}, t) = A^{ext}(\mathbf{r}, t) + \frac{\mu_0}{4\pi} \int \frac{J_T(\mathbf{r}', t - \frac{|\mathbf{r} - \mathbf{r}'|}{c})}{|\mathbf{r} - \mathbf{r}'|} dV'. \quad (1)$$

From here on, we use notation $t_{ret} \equiv t - \frac{|\mathbf{r} - \mathbf{r}'|}{c}$. Focusing only on the scattered radiation and leaving aside polarization, the expression can be rewritten for the special

case of two-level system as:

$$A^{sca}(\mathbf{r}, t) = \frac{\mu_0}{4\pi} \int \frac{\langle e|J|g\rangle(\mathbf{r}', t_{ret})}{|\mathbf{r} - \mathbf{r}'|} \sigma^+(t_{ret}) + \frac{\langle g|J|e\rangle(\mathbf{r}', t_{ret})}{|\mathbf{r} - \mathbf{r}'|} \sigma^-(t_{ret}) dV'$$

where $|g\rangle$ and $|e\rangle$ are to be understood as eigenfunctions of a $H_0 = H_{kin} + V(r)$ Hamiltonian, and the Pauli operators as $\sigma^+ = c_e^\dagger c_g$, $\sigma^- = c_g^\dagger c_e$, and the current density is written as:

$$\langle j|J|i\rangle(\mathbf{r}, t) = -\frac{e\hbar}{2im} (\psi_j^*(\mathbf{r}) \nabla \psi_i(\mathbf{r}) - \psi_i(\mathbf{r}) \nabla \psi_j^*(\mathbf{r})) - \frac{e^2}{m} A(\mathbf{r}, t) \psi_i(\mathbf{r}) \psi_j^*(\mathbf{r}). \quad (2)$$

One can then use the fact that $[\mathbf{r}, H_0] = -\frac{\hbar^2}{m} \nabla$, then for the far-field scattered radiation we can write:

$$A^{sca}(\mathbf{r}, t) \approx \frac{\mu_0}{4\pi} \left(\frac{\int \langle e|J|g\rangle(\mathbf{r}', t_{ret}) dV'}{|\mathbf{r}|} \sigma^+(t_{ret}) + \frac{\int \langle g|J|e\rangle(\mathbf{r}', t_{ret}) dV'}{|\mathbf{r}|} \sigma^-(t_{ret}) \right),$$

which can be simplified further by invoking the dipole-approximation:

$$\begin{aligned} \int \langle j|J|i\rangle(\mathbf{r}, t) dV &\approx \frac{e}{2i\hbar} \int (\psi_j^*(\mathbf{r}) [\mathbf{r}, H_0] \psi_i(\mathbf{r}) - \psi_i(\mathbf{r}) [\mathbf{r}, H_0] \psi_j^*(\mathbf{r})) dV - \frac{e^2}{m} A(\mathbf{0}, t) \int \psi_i(\mathbf{r}) \psi_j^*(\mathbf{r}) dV \\ &= \frac{\epsilon_j - \epsilon_i}{i\hbar} \int \psi_j^*(\mathbf{r}) (-e\mathbf{r}) \psi_i(\mathbf{r}) dV = -i\omega_{ij} d_{ij}. \end{aligned} \quad (3)$$

It needs to be noted that the dipole-approximation is not necessarily acceptable, however if the eigenfunctions are known, calculation of the neglected term is straightforward. Then the far-field vector potential is approximately written as:

$$A^{sca}(\mathbf{r}, t) \approx \frac{\mu_0 \omega_0 d}{4\pi |\mathbf{r}|} \sigma_y(t_{ret}). \quad (4)$$

For the evolution of the localised source, we will consider the Hamiltonian to be independent of spatial coordinates, and neglect the effects due to the propagation of the field, due to the very short interaction time. Let us consider the following terms:

$$H_a = \hbar \frac{\omega_0}{2} \sigma_z, \quad H_m = \sum_n \hbar \omega_n a_n^\dagger a_n, \quad (5)$$

$$H_{am} = \sum_n \hbar \frac{\Omega_n}{2} \sigma_x (a_n + a_n^\dagger), \quad (6)$$

which corresponds to the two-level atom, the quantized electromagnetic modes, and the quantized dipole-interaction corresponds in this order. Since the strong

external exciting pulse can be described classically, we use:

$$H_{ex}(t) = -DE(t) = -d\sigma_x E(t) = -\hbar \frac{\Omega(t)}{2} \sigma_x. \quad (7)$$

We note that $\Omega_n = 2d\sqrt{\frac{\hbar\omega_n}{\epsilon_0 V}}$, where V is the quantization volume. Let us denote the eigenstates of the atomic Hamiltonian by $|e\rangle$ and $|g\rangle$, i.e., $H_a|e\rangle = \hbar\omega_0/2|e\rangle$, $H_a|g\rangle = -\hbar\omega_0/2|g\rangle$.

Utilizing the dipole-approximation, we are led to the following system [1]:

$$H(t) = H_a + H_m + H_{am} + H_{ex}(t), \quad (8)$$

which we solve first.

III. MEASURE OF SQUEEZING

We use the following notations:

$$\begin{aligned} X_n &= \frac{a_n^\dagger + a_n}{2}, & Y_n &= i \frac{a_n^\dagger - a_n}{2} \\ X_{2n} &= \frac{a_n^{\dagger 2} + a_n^2}{2}, & Y_{2n} &= i \frac{a_n^{\dagger 2} - a_n^2}{2} \end{aligned}$$

Squeezed states are associated to canonical observables, in quantum optics typically electric field strength at a given θ phase. The corresponding dimensionless X_n^θ and Y_n^θ operators are defined as:

$$\begin{aligned} X_n^\theta &= \frac{a_n + a_n^\dagger}{2} \cos \theta + i \frac{a_n^\dagger - a_n}{2} \sin \theta, \\ Y_n^\theta &= -\frac{a_n + a_n^\dagger}{2} \sin \theta + i \frac{a_n^\dagger - a_n}{2} \cos \theta, \end{aligned}$$

and for the sake of completeness, we write out the quadratic variances as:

$$\begin{aligned} \langle (\Delta X^\theta)^2 \rangle &= \frac{1}{4} \left(1 + 2\langle N \rangle + 2\langle X_2 \rangle - 4\langle X \rangle^2 \right) \cos^2 \theta \\ &\quad + \frac{1}{4} \left(1 + 2\langle N \rangle - 2\langle X_2 \rangle - 4\langle Y \rangle^2 \right) \sin^2 \theta \\ &\quad + \left(\langle Y_2 \rangle - 2\langle Y \rangle \langle X \rangle \right) \cos \theta \sin \theta, \\ \langle (\Delta Y^\theta)^2 \rangle &= \frac{1}{4} \left(1 + 2\langle N \rangle + 2\langle X_2 \rangle - 4\langle X \rangle^2 \right) \sin^2 \theta \\ &\quad + \frac{1}{4} \left(1 + 2\langle N \rangle - 2\langle X_2 \rangle - 4\langle Y \rangle^2 \right) \cos^2 \theta \\ &\quad - \left(\langle Y_2 \rangle - 2\langle Y \rangle \langle X \rangle \right) \cos \theta \sin \theta. \end{aligned}$$

Quadrature amplitudes are typically measured with balanced homodyne detectors. Measurements are performed on an ensemble of identical states, and quasi-probability density functions are calculated from the data.

Light is considered squeezed, if there exists a mode n and phase θ [4, 20] such that $\Delta X_n^\theta < \frac{1}{2}$. The minimal variance (and its associated phase) can be calculated through the smaller eigenvalue (and associated eigenvector) of the noise-ellipse matrix:

$$\begin{pmatrix} \langle(\Delta X)^2\rangle & \frac{1}{2}\langle\{\Delta X, \Delta Y\}\rangle \\ \frac{1}{2}\langle\{\Delta X, \Delta Y\}\rangle & \langle(\Delta Y)^2\rangle \end{pmatrix} \quad (9)$$

The eigenvalues [15] and eigenvectors [14], expressed with our notations are:

$$\lambda_{\pm} = \frac{1}{4} \left[\langle\{\Delta a, \Delta a^\dagger\}\rangle \pm 2|\langle(\Delta a)^2\rangle| \right] \\ = \frac{1}{4} \left[1 + 2(\langle N \rangle - \langle X \rangle^2 - \langle Y \rangle^2) \pm 2|\langle X_2 + iY_2 \rangle - \langle X + iY \rangle^2| \right], \quad (10)$$

and $\begin{pmatrix} u_1 \\ u_2 \end{pmatrix}$ with the components fulfilling:

$$(u_{\pm})_1^2 = \frac{(\lambda_{\pm} - \langle 2X_2 + 2N + 1 \rangle - 4\langle Y \rangle^2)^2}{(\lambda_{\pm} - \langle 2X_2 + 2N + 1 \rangle - 4\langle Y \rangle^2)^2 + \langle 2Y_2 - 4\langle X \rangle \langle Y \rangle \rangle^2} \\ (u_{\pm})_2^2 = \frac{\langle 2Y_2 - 4\langle X \rangle \langle Y \rangle \rangle^2}{(\lambda_{\pm} - \langle 2X_2 + 2N + 1 \rangle - 4\langle Y \rangle^2)^2 + \langle 2Y_2 - 4\langle X \rangle \langle Y \rangle \rangle^2}. \quad (11)$$

IV. TIME-EVOLUTION OF NEAR-FIELD QUANTITIES

In order to process calculations involving many quantized modes, we will implement a system of dynamical equations describing the time-evolution of expectation values. Due to the nonlinearity of the operator-equations, one needs to introduce a hierarchy of equations involving a factorization of expectation values that is physically acceptable.

In the following, we will use notation:

$$U = \sigma_x, \quad V = -\sigma_y, \quad W = \sigma_z; \quad (12)$$

$$U_n^\pm = (i)^{(1\mp 1)/2} \sigma_x (a_n \pm a_n^\dagger), \\ V_n^\pm = -(i)^{(1\mp 1)/2} \sigma_y (a_n \pm a_n^\dagger), \\ W_n^\pm = (i)^{(1\mp 1)/2} \sigma_z (a_n \pm a_n^\dagger). \quad (13)$$

The quantized electromagnetic field is approximated with discrete modes, with appropriate cutoff, and with frequency-independent mode-density distribution.

We will neglect cross-mode correlations and atomic-high order field correlations, implying $\langle a_i^{(\dagger)} a_j^{(\dagger)} \rangle = \langle a_i^{(\dagger)} \rangle \langle a_j^{(\dagger)} \rangle$ if $i \neq j$ and $\langle \sigma_i N_i \rangle = \langle \sigma_i \rangle \langle N_i \rangle$. Numerical investigations imply that these approximations are acceptable [1] as long as the photon number expectation

values are reasonably small. The resulting dynamical equations can be seen in Appendix A.

We can summarize the dynamics of the quadrature-variances in the following way: the principal variances (λ_{\pm} oscillate in time, with periods that depends on the frequency of the mode).

We note that in harmonic modes (emitted by a single system) the excitation is individually very low. Due to this, even though it is possible to define phase $\phi \equiv \text{atan2}(\langle X \rangle, \langle Y \rangle)$ and $\langle(\Delta X^\phi)^2\rangle$; $\langle(\Delta Y^\phi)^2\rangle$, it is not correct to identify these as amplitude-; or phase-variances.

In order to investigate the quadrature-variances, we have used the minimal (λ_-) and maximal (λ_+) variances. As illustrated on Fig.1, both even and odd harmonics display squeezing in certain time-intervals, with the even harmonic generally being squeezed more often. Maximal variance falls within the same order of magnitude as the photon-number expectation value.

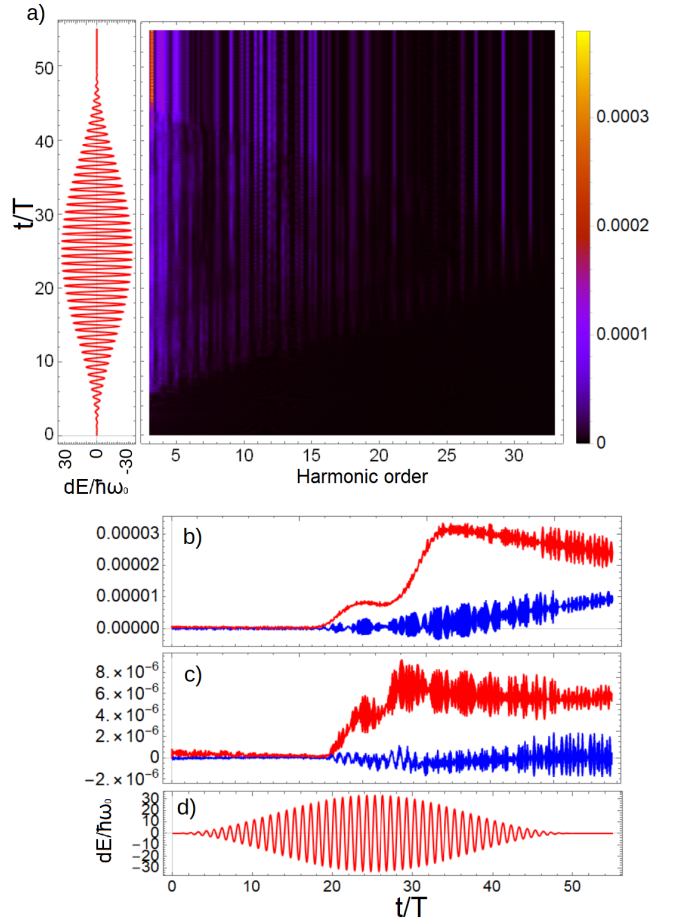


FIG. 1: **a)** Time-evolution of the photon numbers as function of time (vertical axis) and frequency (horizontal axis). **b)** and **c)** show $\lambda_+ - \frac{1}{4}$ (red), and $\lambda_+ - \frac{1}{4}$ (blue) variances of an odd and even harmonic respectively. **d)** shows time-dependence of the excitation. The horizontal axis is shared in **b)** – **d)**.

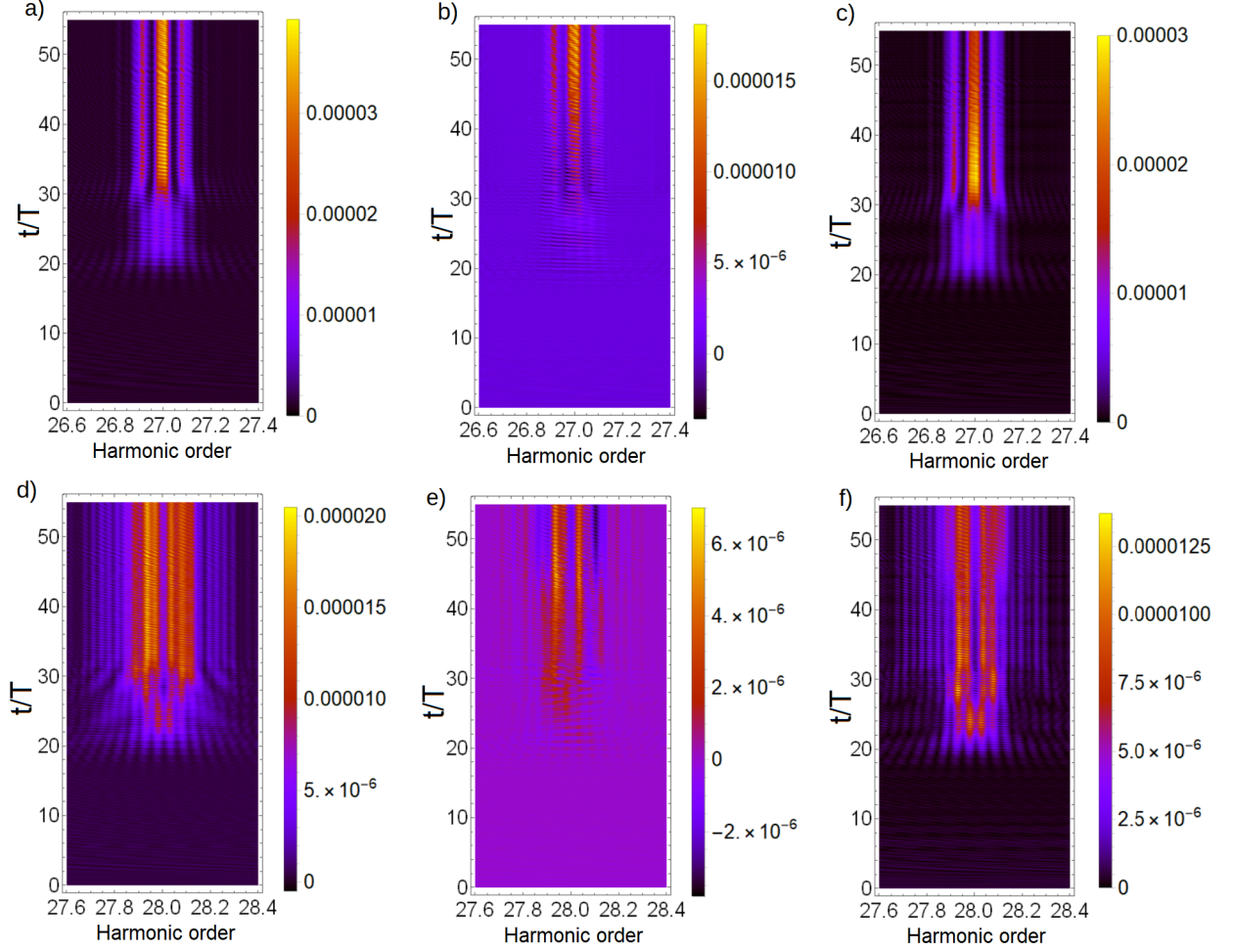


FIG. 2: Magnified view of the dynamics of the 27th and 28th harmonics. **a)** and **d)** shows $\langle N \rangle$ photon-number expectation values; **b)** and **e)** shows $\lambda_- - \frac{1}{4}$; **c)** and **f)** are plots of $\lambda_+ - \frac{1}{4}$.

V. EVOLUTION OF THE SCATTERED ATTOSECOND PULSE

In interaction of generated attosecond pulses with matter, usually the far-field radiation plays important role. The measurement of the electric field at a space-time point would require placing a –not completely localized– test charge at that point. For the description of the field-charge interaction, a spatial mean-field operator [11] can be introduced, essentially equivalent with introducing a cutoff at high frequencies.

The electric field operator of the far-field scattered radiation can be written as $E^{sca} = -\frac{\partial}{\partial t} A^{sca}$. Using notation $C(\mathbf{r}) \equiv \frac{\mu_0 \omega_0 d}{4\pi |\mathbf{r}|}$, it follows that the mean electric field

is:

$$\langle E(\mathbf{r}, t) \rangle = C(\mathbf{r}) \left(-\omega_0 \langle U(t_{ret}) \rangle + \Omega(t_{ret}) \langle W(t_{ret}) \rangle + \sum_n \Omega_n \langle W_n^\dagger(t_{ret}) \rangle \right),$$

while the expectation value of the square of the electric field is:

$$\begin{aligned} \langle E^2(\mathbf{r}, t) \rangle = C^2(\mathbf{r}) & \left(\omega_0^2 + \Omega^2(t_{ret}) \right. \\ & + 2\Omega(t_{ret}) \sum_n \Omega_n \langle X_n(t_{ret}) \rangle \\ & + \sum_n \Omega_n^2 \langle 1 + 2N_n(t_{ret}) + 2X_{2n}(t_{ret}) \rangle \\ & \left. + \sum_{n \neq m} 8\Omega_n \Omega_m \langle X_n(t_{ret}) X_m(t_{ret}) \rangle \right). \end{aligned} \quad (14)$$

The electric-field operator can be divided into semiclassical terms, and terms that are only present due to the model containing quantized electromagnetic modes. The latter terms are those which contain Rabi-frequencies, and can cause noticeable deviation in the electric-field variance if the coupling is strong, or the mode-density is high. Comparison between the semiclassical approximation with our result can be observed on subfigure b) of Fig.([?]). The presence of quantized electromagnetic modes generally increase variance of the electric field.

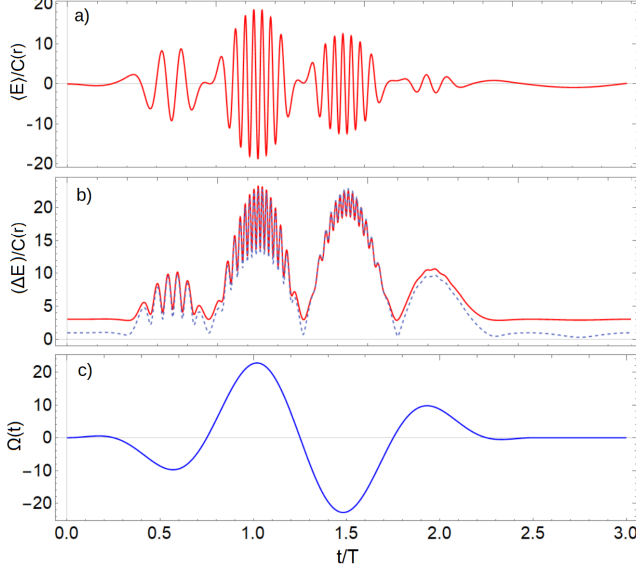


FIG. 3: Time-dependence of: **a)** the scattered electric field mean value; **b)** variance of the scattered electric field with (red) and without (blue) quantized modes; **c)** the excitation. The horizontal axis is shared.

VI. CONCLUSIONS

We have given a set of equations, with which the time-evolution of photon numbers as well as quadrature-amplitudes and variances can be followed simultaneously for a fundamental system in the near-field. Our calculations suggest weak squeezing in individual high harmonics emitted by a single radiating system. This can serve as additional information for the characterization of high harmonics and of attosecond pulses.

We wish to point out that the calculations in this paper

can be generalized to multi-level systems in a straightforward manner.

Acknowledgments

Our work was supported by the Hungarian National Research, Development and Innovation Office under Contracts No. 81364 and K16-120615. Partial support by the ELI-ALPS project is also acknowledged. The ELI-ALPS project (GOP-1.1.1-12/B-2012-000, GINOP-2.3.6-15-2015-00001) is supported by the European Union and co-financed by the European Regional Development Fund.

Appendix A: Dynamical equations

The dynamical equations used in the calculations are listed below:

$$\langle \dot{N}_n \rangle = \frac{\Omega_n}{2} \langle U_n^- \rangle$$

$$\langle \dot{U} \rangle = \omega_0 \langle V \rangle$$

$$\langle \dot{V} \rangle = -\omega_0 \langle U \rangle + \Omega(t) \langle W \rangle + \sum_n \Omega_n \langle W_n^+ \rangle$$

$$\langle \dot{W} \rangle = -\Omega(t) \langle V \rangle - \sum_n \Omega_n \langle V_n^+ \rangle$$

$$\langle \dot{U}_n^+ \rangle = \omega_0 \langle V_n^+ \rangle - \omega_n \langle U_n^- \rangle$$

$$\langle \dot{U}_n^- \rangle = \omega_0 \langle V_n^- \rangle + \omega_n \langle U_n^+ \rangle + \Omega_n$$

$$\begin{aligned} \langle \dot{V}_n^+ \rangle &= -\omega_0 \langle U_n^+ \rangle - \omega_n \langle V_n^- \rangle + \Omega(t) \langle W_n^+ \rangle \\ &+ \Omega_n \langle W \rangle (1 + 2\langle N_n \rangle + 2\langle X_{2n} \rangle) + \sum_{j \neq n} 2\Omega_j \langle W_n^+ \rangle \langle X_j \rangle \end{aligned}$$

$$\begin{aligned} \langle \dot{V}_n^- \rangle &= -\omega_0 \langle U_n^- \rangle + \omega_n \langle V_n^+ \rangle + \Omega(t) \langle W_n^- \rangle \\ &- 2\Omega_n \langle W \rangle \langle Y_{2n} \rangle - 2 \sum_{j \neq n} \Omega_j \langle W_n^- \rangle \langle X_j \rangle \end{aligned}$$

$$\langle \dot{W}_n^+ \rangle = -\omega_n \langle W_n^- \rangle - \Omega(t) \langle V_n^+ \rangle$$

$$- \Omega_n \langle V \rangle (1 + 2\langle N_n \rangle + 2\langle X_{2n} \rangle) - 2 \sum_{j \neq n} \Omega_j \langle V_n^+ \rangle \langle X_j \rangle$$

$$\langle \dot{W}_n^- \rangle = \omega_n \langle W_n^+ \rangle - \Omega(t) \langle V_n^- \rangle + 2\Omega_n \langle V \rangle \langle Y_{2n} \rangle$$

$$- 2 \sum_{j \neq n} \Omega_j \langle V_n^- \rangle \langle X_j \rangle$$

$$\langle \dot{X}_n \rangle = \omega_n \langle Y_n \rangle$$

$$\langle \dot{Y}_n \rangle = -\frac{\Omega_n}{2} \langle U \rangle - \omega_n \langle X_n \rangle$$

$$\langle \dot{X}_{2n} \rangle = -\frac{\Omega_n}{2} \langle U_n^- \rangle + 2\omega_n \langle Y_{2n} \rangle$$

$$\langle \dot{Y}_{2n} \rangle = -\frac{\Omega_n}{2} \langle U_n^+ \rangle - 2\omega_n \langle X_{2n} \rangle$$

- [1] Ákos Gombkötő, Attila Czirják, Sándor Varrò, and Péter Földi. Quantum-optical model for the dynamics of high-order-harmonic generation. *Phys. Rev. A*, 94:013853, 2016.
- [2] Robert Boyd, Svetlana Lukishova, and Victor Zadkov. *Quantum Photonics: Pioneering Advances and Emerging Applications (Springer Series in Optical Sciences 217)*. 02 2019. ISBN 978-3-319-98402-5. doi: 10.1007/

978-3-319-98402-5.

- [3] Gerd Breitenbach, Fabrizio Illuminati, Stephan Schiller, and Jurgen Mlynek. Broadband detection of squeezed vacuum: A spectrum of quantum states. *EPL*, 44:192, 01 2007. doi: 10.1209/epl/i1998-00456-2.
- [4] Matthew Collett and D. Walls. Squeezing spectra for nonlinear optical systems. *Phys. Rev. A*, 32, 12 1985. doi: 10.1103/PhysRevA.32.2887.

- [5] Gy. Farkas and Cs. Tóth. Proposal for attosecond light pulse generation using laser induced multiple-harmonic conversion processes in rare gases. *Phys. Lett. A*, 168(5): 447 – 450, 1992.
- [6] M Ferray, A L’Huillier, X F Li, L A Lompre, G Mainfray, and C Manus. Multiple-harmonic conversion of 1064 nm radiation in rare gases. *J. Physics B*, 21(3):L31, 1988.
- [7] J. Gea-Banacloche. Two-photon absorption of nonclassical light. *Phys. rev. lett.*, 62:1603–1606, 05 1989. doi: 10.1103/PhysRevLett.62.1603.
- [8] J. N. Heyman, K. Craig, B. Galdrikian, M. S. Sherwin, K. Campman, P. F. Hopkins, S. Fafard, and A. C. Gosard. Resonant harmonic generation and dynamic screening in a double quantum well. *Phys. Rev. Lett.*, 72:2183–2186, Apr 1994.
- [9] T. Iskhakov, Maria Chekhova, and Gerd Leuchs. Generation and direct detection of broadband mesoscopic polarization-squeezed vacuum. *Phys. Rev. Lett.*, 102: 183602, 06 2009. doi: 10.1103/PhysRevLett.102.183602.
- [10] L. V. Keldysh. Ionization in the field of a strong electromagnetic wave. *Sov. Phys. JETP*, 20:1307, 1964.
- [11] Ole Keller. *Quantum Theory of Near-Field Electrodynamics*. 08 2011. ISBN 978-3-642-17409-4. doi: 10.1007/978-3-642-17410-0_25.
- [12] Ferenc Krausz and Misha Ivanov. Attosecond physics. *Rev. Mod. Phys.*, 81:163–234, Feb 2009.
- [13] M. Lewenstein, Ph. Balcou, M. Yu. Ivanov, Anne L’Huillier, and P. B. Corkum. Theory of high-harmonic generation by low-frequency laser fields. *Phys. Rev. A*, 49:2117–2132, Mar 1994.
- [14] A. Lukš, V. Peřinová, and J. Peřina. Principal squeezing of vacuum fluctuations. *Opt. Commun.*, 67:149–151, 06 1988. doi: 10.1016/0030-4018(88)90322-7.
- [15] Jan Peřina. *Quantum Statistics of Linear and Nonlinear Optical Phenomena*. Springer, 01 1991. doi: 10.1007/978-94-011-2400-3.
- [16] E. Polzik, J Carri, and H. Kimble. Spectroscopy with squeezed light. *Phys. Rev. Lett.*, 68:3020–3023, 06 1992. doi: 10.1103/PhysRevLett.68.3020.
- [17] C. Riek, P. Sulzer, M. Seeger, A. S. Moskalenko, G. Burkard, D. V. Seletskiy, and A. Leitenstorfer. Subcycle quantum electrodynamics. *Nature*, 541:376–379, 2017.
- [18] Yaakov Shaked, Yoad Michael, Rafi Vered, Leon Bello, M. Rosenbluh, and Avi Pe’er. Lifting the bandwidth limit of optical homodyne measurement. *Nat. Commun.*, 9, 01 2018.
- [19] Nicolas Treps, Nicolai Grosse, Warwick P. Bowen, Claude Fabre, Hans-A. Bachor, and Ping Koy Lam. A quantum laser pointer. *Science*, 301:940–943, 08 2003.
- [20] D. F. Walls and G. J. Milburn. *Quantum Optics*. Springer-Verlag, Berlin, 1994.
- [21] Mingqing Xiao, Ling-An Wu, and H. Kimble. Precision measurement beyond the shot-noise limit. *Phys. Rev. Lett.*, 59:278–281, 08 1987. doi: 10.1103/PhysRevLett.59.278.